



**U.S. ARMY COMBAT CAPABILITIES DEVELOPMENT COMMAND
CHEMICAL BIOLOGICAL CENTER**

ABERDEEN PROVING GROUND, MD 21010-5424

CCDC CBC TR-1566

**Effect of Homoserine Lactones
on the Physical Properties
of Bacterial Nanocellulose Materials**

**Rabih E. Jabbour
Erik Emmons
Ashish Tripathi**

RESEARCH AND TECHNOLOGY DIRECTORATE

Kurt Kunkel

**UNIVERSITY OF MARYLAND
BIOENGINEERING DEPARTMENT
College Park, MD 20742-5025**

July 2019

Disclaimer

The findings in this report are not to be construed as an official Department of the Army position unless so designated by other authorizing documents.

REPORT DOCUMENTATION PAGE

Form Approved
OMB No. 0704-0188

Public reporting burden for this collection of information is estimated to average 1 h per response, including the time for reviewing instructions, searching existing data sources, gathering and maintaining the data needed, and completing and reviewing this collection of information. Send comments regarding this burden estimate or any other aspect of this collection of information, including suggestions for reducing this burden to Department of Defense, Washington Headquarters Services, Directorate for Information Operations and Reports (0704-0188), 1215 Jefferson Davis Highway, Suite 1204, Arlington, VA 22202-4302. Respondents should be aware that notwithstanding any other provision of law, no person shall be subject to any penalty for failing to comply with a collection of information if it does not display a currently valid OMB control number. **PLEASE DO NOT RETURN YOUR FORM TO THE ABOVE ADDRESS.**

1. REPORT DATE (DD-MM-YYYY) XX-07-2019		2. REPORT TYPE Final		3. DATES COVERED (From - To) Oct 2017–Sep 2018	
4. TITLE AND SUBTITLE Effect of Homoserine Lactones on the Physical Properties of Bacterial Nanocellulose Materials				5a. CONTRACT NUMBER	
				5b. GRANT NUMBER	
				5c. PROGRAM ELEMENT NUMBER 91A	
6. AUTHOR(S) Jabbour, Rabih E.; Emmons, Erik; Tripathi, Ashish (CCDC CBC); and Kunkel, Kurt (University of Maryland)				5d. PROJECT NUMBER	
				5e. TASK NUMBER	
				5f. WORK UNIT NUMBER	
7. PERFORMING ORGANIZATION NAME(S) AND ADDRESS(ES) Director, CCDC CBC, ATTN: FCDD-CBR-ID//CBR-IS, APG, MD 21010-5424 University of Maryland, Bioengineering Department; 1101 Main Administration Bldg., College Park, MD 20742-5025				8. PERFORMING ORGANIZATION REPORT NUMBER CCDC CBC-TR-1566	
9. SPONSORING / MONITORING AGENCY NAME(S) AND ADDRESS(ES) CCDC CBC In-House Laboratory Independent Research, Office of the Assistant Secretary of the Army for Acquisition, Logistics and Technology; Pentagon, Washington, DC 22202				10. SPONSOR/MONITOR'S ACRONYM(S) ILIR-ASA(ALT)	
				11. SPONSOR/MONITOR'S REPORT NUMBER(S)	
12. DISTRIBUTION / AVAILABILITY STATEMENT Approved for public release: distribution unlimited.					
13. SUPPLEMENTARY NOTES Since February 2019, the U.S. Army Edgewood Chemical Biological Center is known as the U.S. Army Combat Capabilities Development Command Chemical Biological Center.					
14. ABSTRACT: Bacterial nanocellulose (BNC) is a remarkably versatile nano-biomaterial. It has wide applications in the medicine, defense, electronics, optics, and food industries. Use of BNC material has several advantages over that of plant cellulose because BNC has high purity and crystallinity, a large surface area, durability, biocompatibility, and is widely used for multifunctional purposes. However, BNC materials can be difficult to manufacture and process into useable forms because BNC pellicles are often not uniform in their composition. This may be the result of cell density heterogeneity, which leads to large clusters of dense cellular growth. We believe that BNC morphology can be controlled through manipulation of the quorum-sensing (QS) pathways of the bacterium. We investigated the fundamental factors that affect the growth of nanocellulose biofilm. The results showed a direct correlation between QS molecules (e.g., homoserine lactones [HSLs]) and the physical properties of the bacterial pellicles. Scanning electron microscope data showed a direct impact of HSL molecules on fiber thickness. These experimental data will enhance our understanding and optimization of the QS molecule signals and expression levels to improve bacterial nanocellulose production and customization.					
15. SUBJECT TERMS					
Bacterial nanocellulose (BNC)		Atomic force microscopy		Material	
Quorum sensing (QS)		Homoserine lactone (HSL)		Biofilm	
Scanning electron microscope (SEM)		Mass spectrometry (MS)			
16. SECURITY CLASSIFICATION OF:			17. LIMITATION OF ABSTRACT	18. NUMBER OF PAGES	19a. NAME OF RESPONSIBLE PERSON
a. REPORT	b. ABSTRACT	c. THIS PAGE			19b. TELEPHONE NUMBER (include area code)
U	U	U	UU	28	Renu B. Rastogi (410) 436-7545

Standard Form 298 (Rev. 8-98)
Prescribed by ANSI Std. Z39.18

Blank

PREFACE

The work described in this report was started in October 2017 and completed in September 2018.

Since February 2019, the U.S. Army Edgewood Chemical Biological Center (Aberdeen Proving Ground, MD) is known as the U.S. Army Combat Capabilities Development Command Chemical Biological Center (CCDC CBC).

The use of either trade or manufacturers' names in this report does not constitute an official endorsement of any commercial products. This report may not be cited for purposes of advertisement.

This report has been approved for public release.

Acknowledgments

The authors acknowledge the following individuals for their hard work and assistance with the execution of this technical program:

- Gregory W. Peterson (CCDC CBC) for his support with scanning electron microscopy, and
- Dr. Augustus W. Fountain (CCDC CBC) for his technical input and program management.

Blank

CONTENTS

	PREFACE	iii
1.	INTRODUCTION	1
2.	MATERIALS AND METHODS.....	2
2.1	Bacterial Strains	2
2.2	Cellulose Production and Purification	2
2.3	Solvent Extraction of HSLs from BNC Pellicles.....	3
2.4	Characterization of Bacterial Proteins from BNC Pellicles.....	3
2.5	LC–MS/MS Analysis of Extracted BNC Supernatants	3
2.6	Protein Database and Database Search Engine.....	4
2.7	Raman Chemical Imaging Spectroscopy Measurements.....	4
2.8	Scanning Electron Microscopy (SEM) Measurement of BNC Pellicles	5
3.	RESULTS AND DISCUSSIONS.....	5
3.1	MS Analysis of Extracted Supernatant from BNC Pellicle	5
3.2	Effect of Growth Time on BNC Pellicle Yield.....	7
3.3	Effect of HSLs on BNC Pellicle Thickness	8
3.4	Raman Chemical Imaging of BNC Pellicles	10
3.5	Effect of HSLs on BNC Pellicle Morphology	11
4.	CONCLUSIONS.....	13
	LITERATURE CITED	145
	ACRONYMS AND ABBREVIATIONS	17

FIGURES

1.	Mass spectral analysis of extracted HSLs: (a) full mass spectrum for the extraction LC-MS/MS analysis, (b) MS/MS spectrum represent the mass spectral signature peaks for DHL, and (c) MS/MS spectrum represent the mass spectral signature peaks for DDHL.....	6
2.	Results of the Universal Protein Resource proteomic tools for the identification of experimental peptides with nonredundant microbial database containing curated gram-positive and -negative bacteria.....	7
3.	Growth stages on BNC pellicle yield: (a) average weight of triplicate samples and (b) static growth over 15 days with the three different layers of BNC pellicles clearly depicted.....	8
4.	Effect of different HSL molecules on BNC pellicle thickness.....	9
5.	Effect of HSL concentrations on BNC pellicle thickness with over 144 h of growth.....	10
6.	Raman chemical imaging showing the effect of different HSL molecules on BNC pellicle thickness: (a) Raman chemical FOV image, (b) normal Raman spectra for corresponding region shown in Figure 3a, and (c) Raman signature region that contains specific Raman shifts for cellulose polymeric material.....	11
7.	SEM analysis of different cultures containing HSLs.....	12
8.	Average diameter of BNC fibers obtained from the SEM data analysis for the different BNC fibers.....	13

EFFECT OF HOMOSERINE LACTONES ON THE PHYSICAL PROPERTIES OF BACTERIAL NANOCELLULOSE MATERIALS

1. INTRODUCTION

Nanocellulose materials can be obtained from two vastly different sources: (1) nanocellulose fibrils can be isolated from plant biomass and (2) nanostructured cellulose can be produced by bacteria from the *Gluconacetobacter* bacterial genus. Bacterial cellulose, referred to as bacterial nanocellulose (BNC), is a remarkable material. BNC chemical and physical properties make it highly useful in the tissue-engineering, medicine, defense, fabric, and electronics industries. On the other hand, plant-based nanocellulose material is costly and laborious to manufacture. In addition, although its small rod-like structures can be used in the production of thin films and other materials, the physical properties of plant-based nanocellulose materials are often slight when compared with those of bacterial-based nanocellulose materials.

BNC is formed at the air media interface of active *Gluconacetobacter xylinus* cultures. BNC nanofibers are synthesized from glucose units by *Acetobacter* cellulose synthase (Acs) operon proteins and are secreted by AcsC and AcsD, forming an interconnected cellulose “pellicle” around the cells.¹⁻³ BNC pellicles are comprised of long cellulose fibrils that intertwine with one another and are free of other chemical compounds (i.e., lignin and pectin). BNC films often demonstrate a higher strength and flexibility than plant-based films.⁴ BNC can be easily modified and functionalized through genetic engineering and synthetic biological approaches.⁵⁻¹¹ However, BNC materials can be difficult to manufacture and process into useable forms. In many instances bacterial cellulose pellicles are not uniform in their composition. This is often due to a heterogeneity of cell density, which leads to large clusters of dense cellular growth. Methods have been developed to circumvent some of these issues, but BNC production abnormalities and irregularities in the pellicles are still encountered. To date, no success has been achieved to control the fibril density and mechanical properties of the film or speed up the rate of production.

Homoserine lactones (HSLs) are vital quorum-sensing (QS) molecules that enable bacterial cells to regulate the growth and behavior of their community. HSLs consist of various acyl side chains of 4–14 carbon atoms and may also contain double bonds. A carbon chain of HSLs can be hydroxylated or oxidized to a carbonyl carbon and thus result in quite different physicochemical properties. HSLs are the most common QS signals in gram-negative bacteria, and they coordinate important temporal events, more specifically the formation of biofilms, in nature and in humans.¹²⁻¹³ Little is known about the correlation between bacterial cellulose production, fibril density, pellicle thickness, and the expression of different HSL QS molecules. Therefore, we will address vital questions related to the proposed hypothesis, such as the kinetic impact of the QS signals of HSLs on the synthesis of bacterial cellulose. The rate of cellulose production is affected at specific time points in the presence or absence of QS molecules. The contribution of each QS molecule to the production of cellulose and its impact on its fibril density and pellicle thickness were investigated.

Before using BNC in various applications, it is imperative that fundamental research is performed to seek the ideal BNC composition for each individual application. There are many factors that could assist the BNC to perform to its maximum potential. For instance, the morphological characterization and physical properties of BNC (i.e., pore size, nanofibers diameter, and density) could affect how well it performs in each application. The objective of our first-year research was to grow the bacterial cellulose under different conditions. This effort included the addition of different HSL-signaling molecules to the growth media of each pellicle. Different concentration levels of the HSL molecules were added. Our initial data showed that the type of HSL molecule affected BNC morphology and physical properties, and HSL concentration affected BNC physical or morphological properties. The data showed that it is possible to correlate the impact of HSLs acting as QS molecules with that of BNC morphological characteristics.

2. MATERIALS AND METHODS

2.1 Bacterial Strains

G. xylinus, a bacterial strain, was used to produce the nanocellulose. It was obtained from the American Type Culture Collection (Manassas, VA) as *G. xylinus* strain 10245, which is cultured in Hestrin–Schramm (HS) medium with 2 wt/vol% glucose. Stock bacterial culture was added to 10 mL of HS media in 50 mL conical tubes and was grown at 27 °C for 3–7 days, depending on the amount of biofilm formation. The growth was conducted under static culture in which no agitation of the culture broth was performed. When the bacterial cellulose biofilm was formed, it was removed for further processing and characterization.

2.2 Cellulose Production and Purification

Bacterial cellulose was formed after approximately 72 h of growth. The formation of bacterial cellulose occurred in static culture; the cells were grown in 50 mL conical tubes containing 10 mL of HS medium at 27 °C for 3–7 days. The cellulose pellicles were then isolated and purified by treating with 0.5% of sodium hydroxide at 100 °C for 1 h before extensive washing with milli-Q (Merck Millipore; Burlington, MD) water to remove excess sodium hydroxide solution and reduce the pH balance. The pellicles were checked periodically during the washing process to ensure that their pH balance was maintained at 4–5. After the pellicles were washed with water, they were dried at 30 °C for 24 h and then weighed on an analytical balance. The mass obtained was normalized to include the culture volume used to compare the pellicle yield obtained by the addition of different HSLs. Cleaned but unprocessed pellicles were kept in 0.1M sodium azide solution.

2.3 Solvent Extraction of HSLs from BNC Pellicles

The extraction of the HSLs for mass spectrometry (MS) analysis was performed in accordance with the method described by Eng et al.:¹⁴

- BNC pellicles were collected;
- the supernatant was centrifuged to remove bacterial cells and any cellular debris at 14,000 rpm for 15 min at a controlled temperature of 4 °C;
- the supernatant was extracted with either 100 or 50% cold methanol solution;
- the extraction step was repeated three times for each of the methanol solutions;
- the extract was allowed to evaporate at room temperature;
- the solutions were resuspended in 2 mL each of milli-Q water and ethyl acetate (3×);
- the ethyl acetate partition was then evaporated, and the residue was resuspended in hexane–ethyl acetate (90:10);
- solid-phase extraction was performed using a silica hydrophilic phase;
- the column was washed with ethyl acetate and then equilibrated with hexane–ethyl acetate solution (90:10);
- a mixture of hexane–ethyl acetate (95:5) solvent was used; and
- the eluted samples were transferred to MS vials for analysis.

2.4 Characterization of Bacterial Proteins from BNC Pellicles

The extracted bacterial suspension from the BNC pellicles was vortexed, and 2 min of lysis was conducted using the bead-beating process. The lysed supernatant was decanted into a new 2 mL tube and centrifuged at 6,600×g (15,000 rpm) for 20 min to pellet the bacterial cells. This was the subsequent protocol for the denaturing and trypsin digestion of the extracted proteins from the BNC pellicles. The resulting tryptic peptides were analyzed using the liquid chromatography tandem mass spectrometry (LC–MS/MS) technique.

2.5 LC–MS/MS Analysis of Extracted BNC Supernatants

The extracted HSLs were separated using a capillary Hypersil C18 column (ThermoFisher Scientific; San Jose, CA; 300 Å, 5 µm, 0.1 mm i.d., and 100 mm in length) with the easy nanoLC from ThermoFisher Scientific. The elution was performed using a linear gradient from 98% A (0.1% of formic acid in water) and 2% B (0.1% of formic acid in acetonitrile) to 60% B over 60 min at a flow rate of 200 nL/min before conducting 20 min of isocratic elution. The resolved analytes were electrosprayed into an orbitrap mass analyzer (Q Exactive Hybrid Quadrupole-Orbitrap; ThermoFisher Scientific) at a flow rate of 200 nL/min. Product ion mass spectra were obtained in the data-dependent acquisition mode that consisted of a survey scan over the mass-to-charge (m/z) range of 400–2000 before conducting a single scan on the most intense precursor ions activated for 30 ms by an excitation energy level of 35%. A dynamic exclusion was activated for 3 min after the first tandem mass spectrometry (MS/MS) spectrum acquisition for a given ion.

2.6 Protein Database and Database Search Engine

A protein database was constructed in a FASTA format using the annotated bacterial proteome sequences derived from fully sequenced chromosomes of all available bacterial strains and more than 120 common laboratory contaminant proteins. We used the PERL programⁱ to download these sequences automatically from the National Center for Biotechnology Information (NCBI; Bethesda, MD) site.ⁱⁱ Each database entry for a given protein sequence has information about a source organism and a genomic position of the respective open-reading frame embedded into a header line. The constructed bacterial proteome database resulted from translating putative protein-coding genes and consists of the corresponding amino acid sequences of potential tryptic peptides from the included bacteria and the common laboratory contaminants. We used COMET¹⁴ (Open Source) to generate the in-silico tryptic peptides, and two missed cleavages were allowed during this latter process.

The experimental MS/MS spectral database of bacterial peptides was searched using the COMET algorithm against the constructed proteome database of microorganisms. The COMET thresholds for searching the product ion mass spectra of peptides were correlation score (Xcorr), relative correlation score (ΔCn), specificity (Sp), relative specificity (RSp), and change in the mass of the peptide ($\Delta Mpep$). The top peptide hits generated by COMET were filtered by $\Delta Cn > 0.1$, and the filtered hits were accepted as peptide identifications when their Xcorrs were higher than the thresholds that allowed a desired false discovery rate (FDR) value to be generated. A protein is identified as present when it is matched with at least two or more validated peptides in an analyzed sample. The ABOid algorithm infers identification of the analyzed sample using assignments of organisms to taxonomic groups (phylogenetic classification) based on an organized scheme that begins at the phylum level and follows through classes, orders, families, and genus, down to the strain level.

2.7 Raman Chemical Imaging Spectroscopy Measurements

The Raman chemical imaging analyses of the BNC samples were taken in Stokes vibrational spectra. The Raman spectroscopy experiments were performed using a Witec (Ulm, Germany) alpha300 R confocal Raman microscopy system. A 100 \times microscope objective in the Raman microscopy was used. A Rayshield (Tempe, AZ) notch filter was used to provide lateral force-resisting system features (from a wavenumber of 10 cm^{-1}). A solid-state laser with a wavelength of 532.1 nm was used. A wavelength of 532 nm was used for excitation, with a power of ~ 2 mW incident on the substrate. The Raman scattered light was collected in the backscattering configuration and transmitted through a 100 μm slit to a 600 grooves/mm grating, which dispersed the light onto a thermoelectrically cooled charge-coupled device camera (Witec DV401 A). A spectral resolution of approximately 5 cm^{-1} was obtained. Spectra were acquired in 5 to 10 s acquisition times. At a lower Raman shift, spurious contributions from the elastic line can be detected by measuring the scattering from a metal surface. On the anti-Stokes side, our spectrometer instrument response was better, which allowed us to measure the Raman spectrum down to 5 cm^{-1} of the Raman shift. The sample image in the entrance spectrometer plane was

ⁱ <http://www.activestate.com/Products/ActivePerl> (accessed April 2018).

ⁱⁱ <http://www.ncbi.nlm.nih.gov> (accessed April 2018).

selected in such a way that the contribution from the glassy slide did not come into the spectrometer. No polarization selection was used.

2.8 Scanning Electron Microscopy (SEM) Measurement of BNC Pellicles

The measurements were performed with a Phenom Pro X (ThermoFisher Scientific) desktop SEM. A beam energy of 15 keV was used to obtain the images. The samples were coated with ~30 nm of gold using a vacuum thermal evaporator system before taking the measurements to reduce charging and beam damage effects from the electron beam. The SEM system was also equipped with energy-dispersive spectroscopy capability to allow for the determination of the elemental content of the analyzed materials.

3. RESULTS AND DISCUSSIONS

3.1 MS Analysis of Extracted Supernatant from BNC Pellicle

The extracted supernatant from the BNC pellicle was analyzed using LC–MS/MS to determine the amount of HSL excreted by the *G. xylinus* during the biofilm formation. Figure 1a–c shows the full mass spectrum of the extracts. Figure 1a shows that there are four major peaks, and these peaks were scanned in MS/MS mode to reveal the chemical structure and infer a chemical identity. Figures 1b and c present the MS/MS spectra for two of the HSLs, namely the decanoyl homoserine lactone (DHL) and the dodecanoyl homoserine lactone (DDHL). The other two HSLs that were identified were hexanoyl and oxydodecanoyl (ODDHL). The HSL identification was achieved through the comparison of their MS/MS spectra with standard spectra for the mentioned compounds. However, it is noteworthy to mention that the MS/MS spectra for the identified HSLs (extracted from the BNC pellicle) had a lower signal-to-noise ratio than that of standard spectra obtained from stock solutions of the same lactone molecules. This could be due to the presence of impurities in the extraction samples, which could be seen in the full mass spectra of these samples. Once these HSLs were identified, we analyzed their stock solutions using the same LC–MS/MS method used to establish a verification of their mass spectra. Moreover, literature showed that these HSLs are also identified in the same strain with the exception of ODDHL, which is reported with near-neighbor strains of the *G. xylinus* (i.e., *Pseudomonas aeruginosa* and *Pseudomonas syringae*).¹⁵

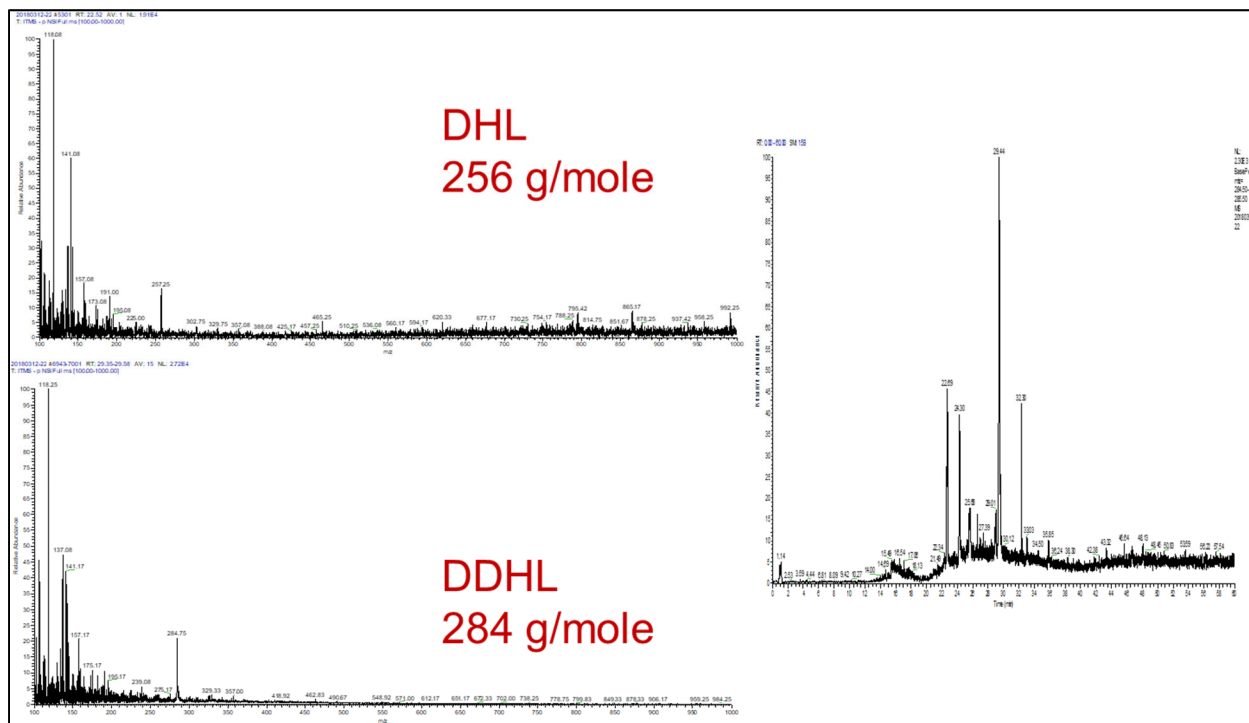


Figure 1. Mass spectral analysis of extracted HSLs: (a) full mass spectrum for the extraction LC–MS/MS analysis, (b) MS/MS spectrum represent the mass spectral signature peaks for DHL, and (c) MS/MS spectrum represent the mass spectral signature peaks for DDHL.

The presence of ODDHL molecules in the *G. xylinus* culture involved a verification of the strain that was present, and this resulted in the analysis of bacterial proteins obtained from processing a lysed bacterial sample of *G. xylinus*. The LC–MS/MS results showed a 95% confidence level matching between our analyzed sample of *G. xylinus* and its public entry at the NCBI depository. This was shown using our in-house algorithm, but we also used a public protein tools consortium to identify the experimental proteins using a nonredundant and nonrestrictive microbial database. Most of the proteins, especially the ones responsible for cellulose and homoserine synthesis, were strain-specific with e-values at 2×10^{-17} and a 100% positive identification match with the experimental sequences. Although cellulose synthase 1 operon protein was present in different BNC-forming strains, some of the strains were unique (i.e., certain sequence alterations made them unique [Figure 2]).^{16–19}

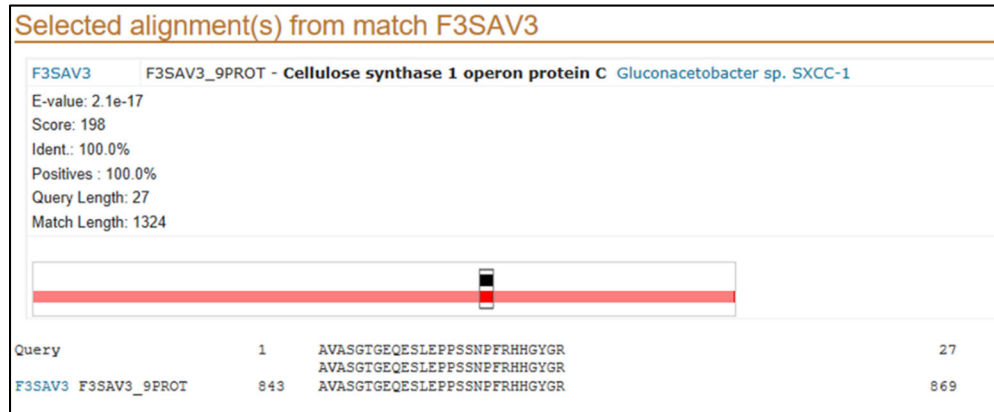


Figure 2. Results of the Universal Protein Resourceⁱⁱⁱ proteomic tools for the identification of experimental peptides with nonredundant microbial database containing curated gram-positive and -negative bacteria.

3.2 Effect of Growth Time on BNC Pellicle Yield

The *G. xylinus* strain was grown in static conditions, and after five days, new culture media was added to the tube that had already formed a BNC pellicle. The new culture media was allowed to grow for another five days before another 5 mL of culture media was added. The solution was then allowed to grow for another five days. The resulting solution contained three distinct layers of BNC pellicles separated by the added media. The higher the layer of the BNC pellicles in the tube, the younger its growth age:

- the bottom layer was 15 days old,
- the middle layer was 10 days old, and
- the top layer was 5 days old.

Figure 3a shows the average weight of the BNC pellicles for each layer. The layers were labelled as (T) for top layer, (M) for middle layer, and (B) for bottom layer. Figure 3b shows a picture of the growth tube that contained the three distinct layers of BNC pellicles separated by the culture media. These results showed that the bottom and middle layers were heavier than the top layer, which could be attributed to the fact that the bottom and middle layers were exposed to culture media from below and above the BNC pellicles, and this provided extra nutrient to form more pellicles. In addition, exposure to more nutrient could produce more bacterial cells that in turn could form more pellicles. The top layer did not have culture media above it and thus, its pellicle formation depended on the amount of the nutrient provided by the layer below the growth media. These data showed a drastic change in the dry weight of the BNC pellicles because of the growth period and the position of the BNC biofilm layer in such static growth conditions. This detail is important for consideration during the growth of BNC pellicles

ⁱⁱⁱ <https://www.uniprot.org/> (accessed April 2018).

and could provide a guide into the growth approach of BNC biofilm depending on the desired production amount and growth time.

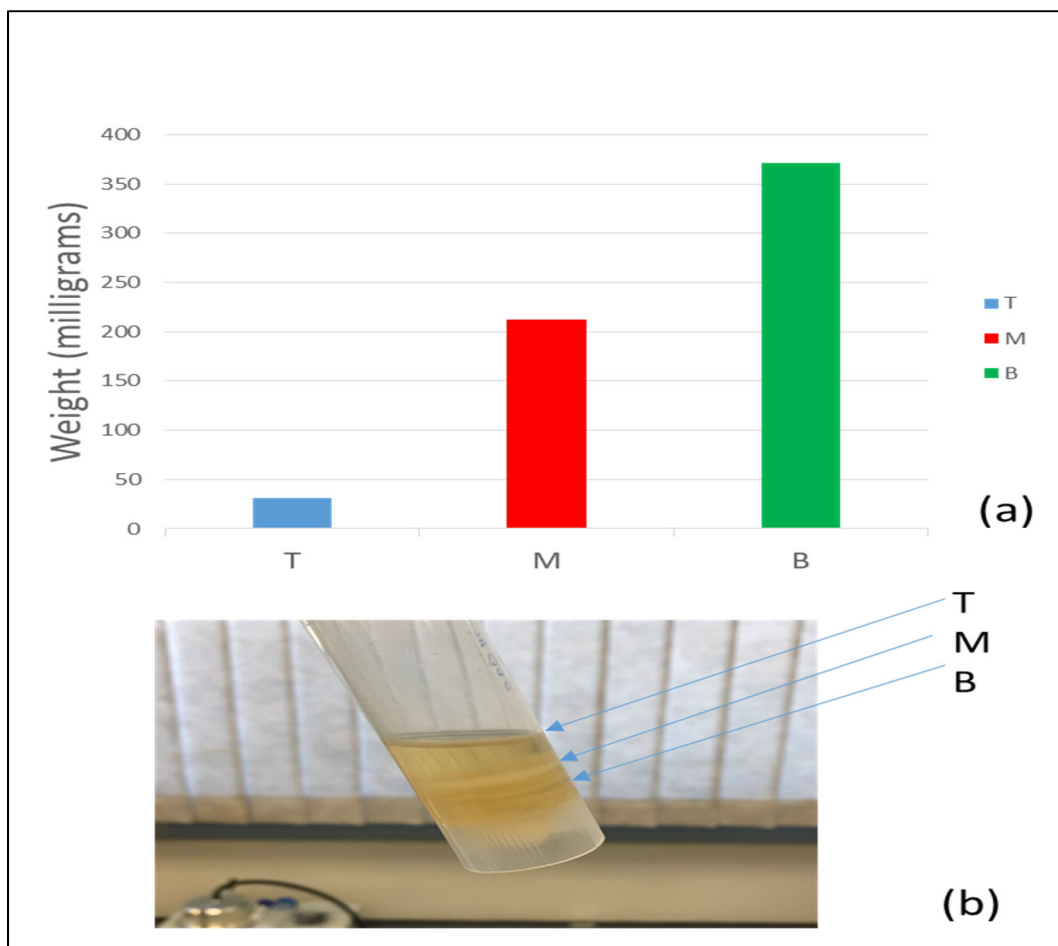


Figure 3. Growth stages on BNC pellicle yield: (a) average weight of triplicate samples and (b) static growth over 15 days with the three different layers of BNC pellicles clearly depicted. (The image was cropped for clarity.)

3.3 Effect of HSLs on BNC Pellicle Thickness

Introduction of different HSLs to the growth media of the BNC pellicles was investigated in terms of the HSL effect on the thickness of the BNC pellicles. We attempted to understand how HSL type could potentially impact the physical properties of BNC pellicles. Measuring the thickness of the BNC pellicles could provide an indication of the potential impact of HSLs on BNC formation. Figure 4 shows the results of introducing four different HSLs to the *G. xylinus* growth media. The thickness of the formed pellicles was measured at different growth times (i.e., 48, 72, and 144 h). The overall trend shows that the maximum increase occurred in the thickness of the pellicle up to 72–96 h, and then, the growth plateaued. The HSLs showed a more significant impact on thickness up to 72 h growth time. Within this time range, the

hexanoyl homo lactones (HXHL) increased pellicle thickness the most, as compared with other lactones, namely the DHL, DDHL, and ODDHL lactones. Although the thickness of the BNC pellicles did not show any measurable increase after 96 h of growth, no change occurred in the order of HSL molecules that provided the highest thickness. Clearly, there was a different impact on the BNC formation based on the HSL type that was infused with the culture media during the growth phase, which could be attributed to the change in morphology of the BNC pellicles. The potential explanation for such behavior could be due to the fact that certain signal molecules could have variable impact on signal transduction during BNC pellicle formation, or a more efficient route could exist for certain HSLs to induce the cells to produce more pellicles. Such an explanation needs to be validated through genetic manipulation of the factors that affect specific HSL production.

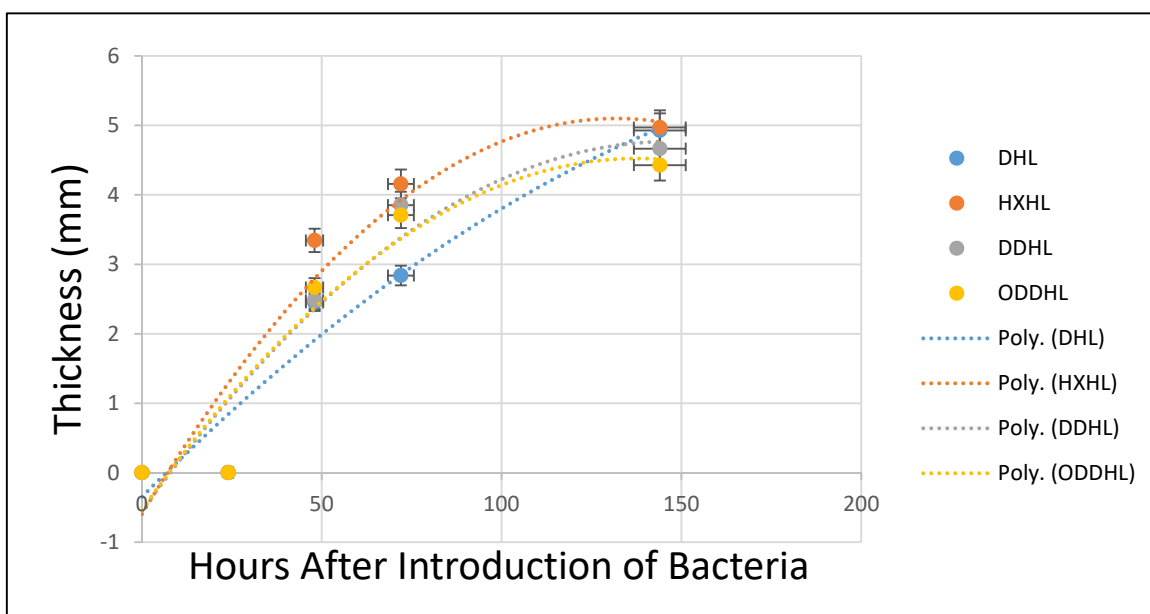


Figure 4. Effect of different HSL molecules on BNC pellicle thickness.

Changing the concentration levels of the added HSLs to the growth media of *G. xylinus* was also investigated. Three different concentration levels were used: 0.1, 0.5, and 1.0 $\mu\text{g}/\text{mL}$. Different HSL concentration levels between 5 and 100 ng were selected for introduction into the growth media in accordance with reported literature.¹⁵ Figure 5 shows the effect of the HSL concentration levels on the thickness of the BNC pellicle and the result obtained from the addition of HXHL. This HSL type was selected because it affected the largest improvement on BNC pellicle thickness when compared with other HSLs (Figure 4). However, the change in the added concentration of HSLs did not significantly affect the thickness of the BNC pellicles (Figure 5). The three data sets differ in the concentration of the signaling molecule. There was no growth until 48 h, and the growth period plateaued after 144 h. There was little difference in the thickness when the concentrations of the pellicles were compared. This could be due to bacterial secretion of sufficient amounts of HSL that are enough to initiate the signal process for the BNC pellicle; therefore, the added amounts of the HSLs were beyond those needed for the regulatory circuits that control BNC pellicle formation. It should be noted

that other HSLs have the same pattern as that of HXHL (data not shown) with no significant change in the thickness of the pellicle, as compared with the standard culture of *G. xylinus* with no added HSLs.

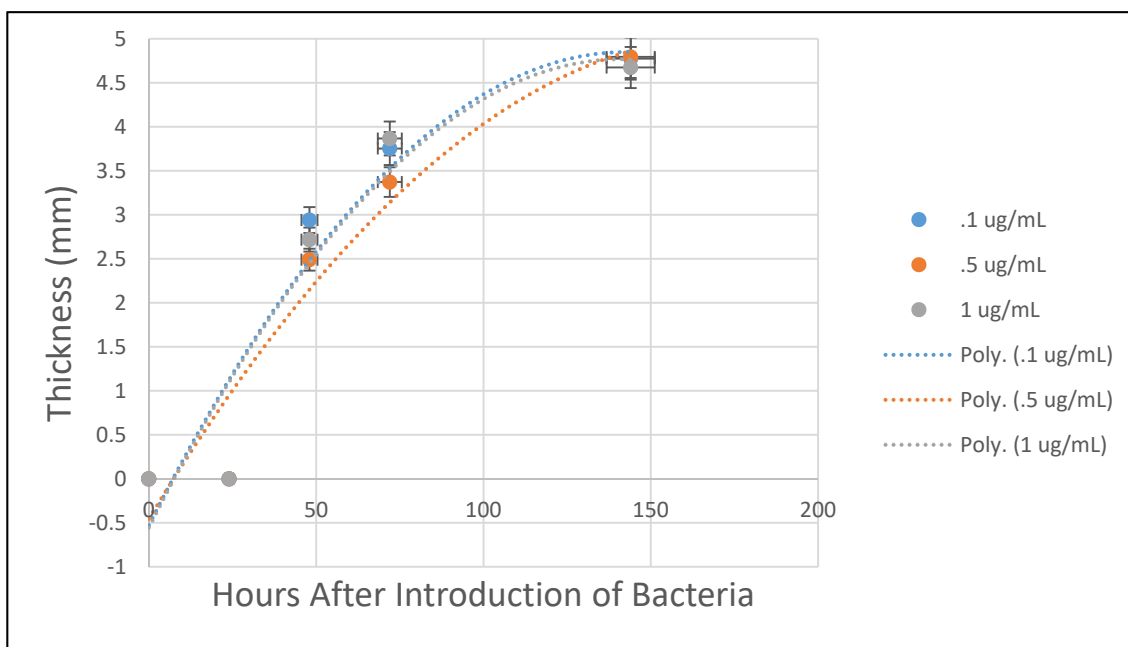


Figure 5. Effect of HSL concentrations on BNC pellicle thickness with over 144 h of growth.

3.4 Raman Chemical Imaging of BNC Pellicles

Raman chemical imaging has been shown to be an effective technique to differentiate the chemical mixture present on a given surface by providing the corresponding Raman shifts that are chemical signatures of presented analytes on a given surface. Moreover, Raman chemical imaging can provide imaging modalities by probing tissues and microorganisms at subcellular resolution, which provide visual output of the morphological and chemical details of the tested samples. Raman chemical imaging was used in this study to verify that the formed BNC pellicles are truly cellulose and can be distinguished from noncellulose fibril materials. Therefore, an aluminum slide was spotted with 5 μL of the BNC pellicle residue and allowed to dry at 27 $^{\circ}\text{C}$ for 2 h. A field of view (FOV) image was scanned at the x,y FOV, and chemical and FOV images were superimposed to provide the montage chemical image in Figure 6a–c. In Figure 6a, a montage Raman chemical image reflects the different constituents deposited from the aluminum slide. Figure 6b shows the corresponding Raman spectra for each region on the aluminum slide. Figure 6c shows the Raman signature region for cellulose material, especially the peaks at 1362 and 1457 cm^{-1} , which are indicative of the presence of a CH₂ band in cellulose polymeric materials, and once a CH₂ band becomes deformed, it will shift toward 1362 cm^{-1} .²⁰ The cellulose signature peaks are not present in the green material located on the cellulose fibrils or in the background region that corresponds to the supernatant material of the BNC pellicle.

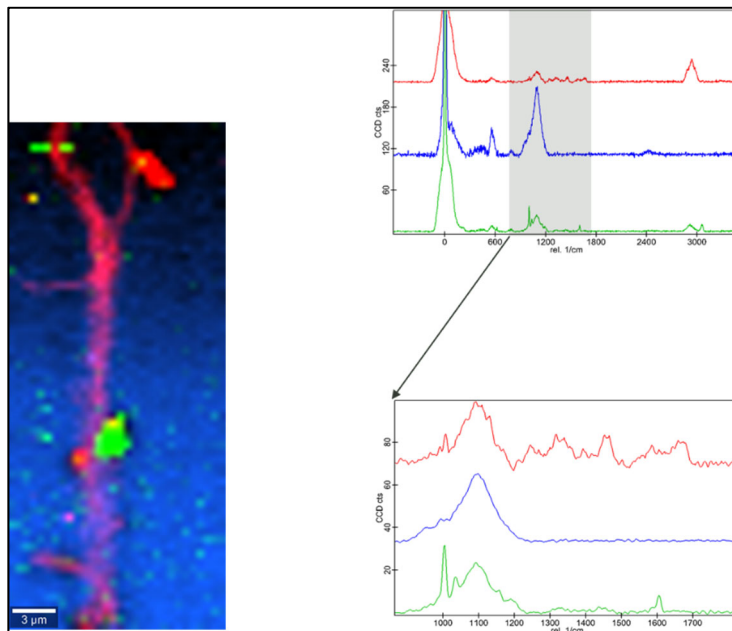


Figure 6. Raman chemical imaging showing the effect of different HSL molecules on BNC pellicle thickness: (a) Raman chemical FOV image, (b) normal Raman spectra for corresponding region shown in Figure 3a, and (c) Raman signature region that contains specific Raman shifts for cellulose polymeric material.

3.5 Effect of HSLs on BNC Pellicle Morphology

Morphological characterization of the BNC pellicle was investigated using SEM technology to determine potential two-dimensional (2D) spatial variation due to the presence of different HSLs in *G. xylinus* growth media. The SEM analysis was used to focus on determining any potential changes in the BNC fiber diameter after the addition of the HSL-signaling molecules. The diameter of the nanofibers was measured by the Fibermetric software program (Adobe, Inc.; San Jose, CA), which was interfaced to a bench-top SEM. We acquired the SEM images for the pellicles at different growth conditions. The SEM images were collected at 15 keV and 1–5 μm resolution. Six different pellicle samples were analyzed in which four had HSL-signaling molecules and two were control samples with no HSL-signaling molecule. Figure 7 shows the output of the SEM measurements with the diameter distributions of the fibers (determined by Fibermetric) as histograms for all the available fibers in the FOV. The diameter sizes for the pellicles with signaling molecules vary, whereas those of the pellicles without signaling molecules do not vary. Moreover, it is noteworthy to point out that when the *G. xylinus* was grown in static mode in a Petri dish filled with a thin layer of growth media (5 mL), it produced a thin film of BNC pellicles. The SEM analysis of this thin film of pellicles showed a nonuniform surface with a sheet-like shape dominating the FOV, which is seen in the standard static mode of growth in the 50 mL conical tubes.

When the average diameter of the BNC fibers was calculated, it was determined that most of the pellicles produced from growth media containing HSLs had a larger average diameter as compared with that of the no-HSL pellicle. However, when the SEM data were compared with the thickness measurements for the same HSLs, a direct correlation could be determined. Figure 8 shows the average diameter of the BNC fibers from different growth phases of the BNC pellicles with different HSLs. Figure 8 shows that most of the added HSLs enlarged the diameter of the fibers without altering its shape or integrity. Although this explanation is based on our experimental data, further experimental investigation of the factors affecting the enlargement of the pellicles in the presence of HSLs are needed. These experiments will address the impact on the micro level of genetic materials responsible for the secretion of HSLs and how such factors, when manipulated, can impact the formation of BNC pellicles. In addition, atomic force microscopy experiments were initiated to provide specific information on the 3-D spatial variation of pellicle morphology. Such experiments are valuable for 3-D surface characterization. They provide a more accurate picture on morphological changes and whether these changes are the direct result of HSL presence in the *G. xylinus* growth media.

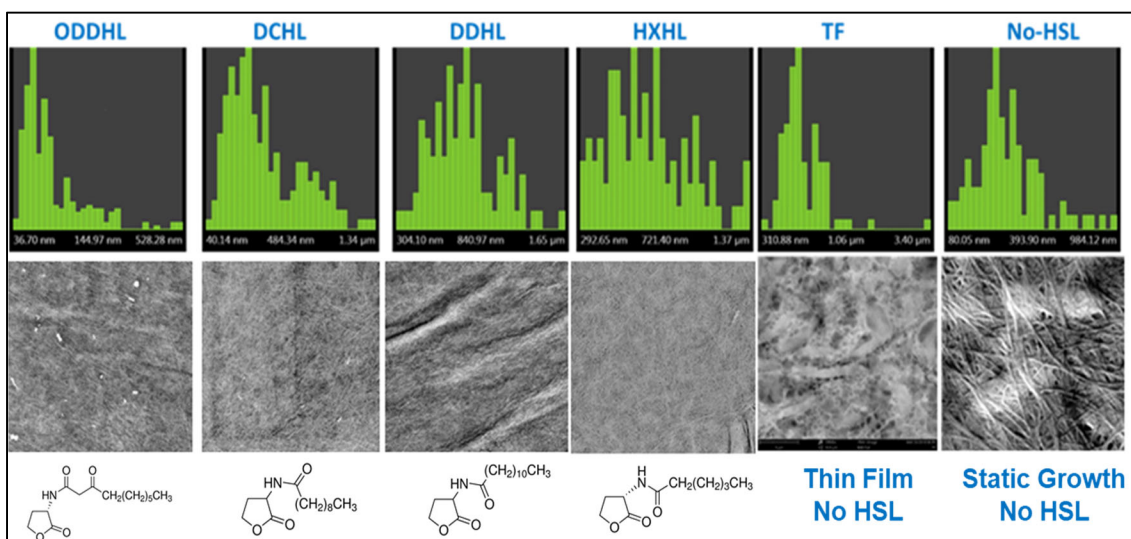


Figure 7. SEM analysis of different cultures containing HSLs. The top panel represents the distribution of the diameter sizes for the FOV of the detected bacterial fibers. The bottom panel represents the SEM images obtained for each BNC pellicle.

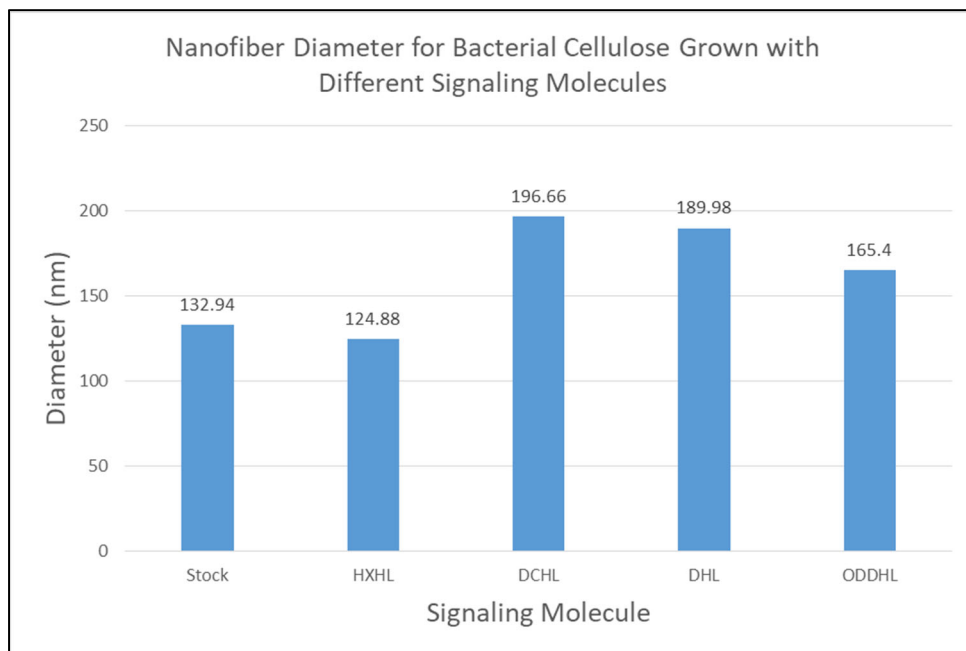


Figure 8. Average diameter of BNC fibers obtained from the SEM data analysis for the different BNC fibers.

4. CONCLUSIONS

The results showed that BNC pellicles can be manipulated using different experimental conditions and that signaling molecules seem to have a direct impact on their physical properties and morphology. More work must be conducted to confirm the present findings; however, these results are useful in understanding the BNC biofilm formation and how its physical properties are affected by QS molecules. More in-depth research into the genetic materials that control the formation and secretion of the HSL-signaling molecules is needed to gain insight into the characteristics of BNC biofilm formation. Although four different HSL molecules were identified, there was no indication that such bacterial strains do not produce different HSL molecules. Modulation of HSL production by regulatory circuits may influence BNC biofilm formation and provide a natural way to produce tailored BNC for certain applications. Identifying and characterizing such a regulatory process may be useful to develop efficient synthetic biological approaches to produce desired BNC biofilms.

Genomic-based experiments will be planned to study the physical properties of BNC pellicles and to give us a better understanding of the BNC biofilm formation mechanism during the secretion of HSL-signaling molecules. This genetic engineering approach will include using specific enzymes such as acyl-HSL synthase that can be altered by functionality to produce different HSL types. Measuring the expression level of such an enzyme is feasible using the LC-MS/MS technique, and comparing its expression level with different BNC-forming bacteria will be valuable in determining the optimal biological system for BNC production.

Blank

LITERATURE CITED

1. Lee, K-Y; Buldum G.; Mantalaris, A.; Bismarck, A. More than Meets the Eye in Bacterial Cellulose: Biosynthesis, Bioprocessing, and Applications in Advanced Fiber Composites. *Macromol. Biosci.* **2014**, *14* (1), 10–32.
2. Rognoli, V.; Bianchini, M.; Maffei, S.; Karana, E. DIY Materials. *Mater. Des.* **2015**, *86*, 692–702.
3. Wong, H.C.; Fear, A.L.; Calhoon, R.D.; Eichinger, G.H.; Mayer, R.; Amikam, D.; Benziman, M.; Gelfand, D.H.; Meade, J.H.; Emerick, A.W. Genetic Organization of the Cellulose Synthase Operon in *Acetobacter xylinum*. *Proc. Natl. Acad. Sci. USA* **1995**, *87* (20), 8130–8134.
4. Williams, W.S.; Cannon, R.E. Alternative Environmental Roles for Cellulose Produced by *Acetobacter xylinum*. *Appl. Environ. Microbiol.* **1989**, *55* (10), 2448–2452.
5. Zhong, C.; Gurry, T.; Cheng, A.A.; Downey, J.; Deng, Z.; Stultz, C.M.; Lu, T.K. Strong Underwater Adhesives Made by Self-Assembling Multiprotein Nanofibres. *Nat. Nanotechnol.* **2014**, *9* (10), 858–866.
6. Chen, A.Y.; Deng, Z.; Billings, A.N.; Seker, U.O.S.; Lu, M.Y.; Citorik, R.J.; Zakeri, B.; Lu, T.K. Synthesis and Patterning of Tunable Multiscale Materials with Engineered Cells. *Nat. Mater.* **2014**, *13* (5), 515–523.
7. Yadav, V.; Paniliatis, B.J.; Shi, H.; Lee, K.; Cebe, P.; Kaplan, D.L. Novel *In Vivo*-Degradable Cellulose-Chitin Copolymer from Metabolically Engineered *Gluconacetobacter xylinus*. *Appl. Environ. Microbiol.* **2010**, *76* (18), 6257–6265.
8. Mohite, B.V.; Patil, S.V. Physical, Structural, Mechanical and Thermal Characterization of Bacterial Cellulose by *G. Hansenii* NCIM 2529. *Carbohydr. Polym.* **2014**, *106*, 132–141.
9. Hsieh, Y.C.; Yano, H.; Nogi, M.; Eichhorn, S.J. An Estimation of Young's Modulus of Bacterial Cellulose Filaments. *Cellulose* **2008**, *15* (4), 507–513.
10. Rusli, R.; Eichhorn, S.J. Determination of the Stiffness of Cellulose Nanowhiskers and the Fiber-Matrix Interface in a Nanocomposite Using Raman Spectroscopy. *Appl. Phys. Lett.* **2008**, *93* (3), 033111.
11. Gelin, K.; Bodin, A.; Gatenholm, P.; Mihranyan, A.; Edwards, K.; Stromme, M. Characterization of Water in Bacterial Cellulose Using Dielectric Spectroscopy and Electron Microscopy. *Polymer* **2007**, *48* (26), 7623–7631.

12. Yuen, J.D.; Walper, S.A.; Melde, B.J.; Daniele, M.A.; Stenger, D.A.; Electrolyte-Sensing Transistor Decals Enabled by Ultrathin Microbial Nanocellulose. *Sci. Rep.* **2017**, *7*, 40867; doi: 10.1038/srep40867.
13. Rudrappa, T.; Biedrzycki, M.L.; Bais, H.P. Causes and Consequences of Plant-Associated Biofilms. *FEMS Microbiol. Ecol.* **2008**, *64*, 153–664.
14. Eng, J.K.; Jahan, T.A.; Hoopmann, M.R. Comet: an Open-Source MS/MS Sequence Database Search Tool. *Proteomics* **2013**, *13*, 22–24.
15. Shaw, P.D.; Ping, G.; Daly, S.L.; Cha, C.; Cronan, J.E.; Rinehart, K.L.; Farrand, S.K. Detecting and Characterizing *N*-acyl-homoserine Lactone Signal Molecules by Thin-Layer Chromatography. *Proc. Natl. Acad. Sci. USA* **1997**, *94* (12), 6036–6041.
16. Saxena, I.M.; Lin, F.C.; Brown, R.M. Cloning and Sequencing of the Cellulose Synthase Catalytic Subunit Gene of *Acetobacter Xylinum*. *Plant Mol. Biol.* **1990**, *15* (5), 673–683.
17. Hense, B.A.; Kuttler, C.; Muller, J.; Rothballer, M.L.; Hartmann, A.; Kreft, J.U. Does Efficiency Sensing Unify Diffusion and Quorum Sensing? *Nat. Rev. Microbiol.* **2007**, *5*, 230–239.
18. Von Rad, U.; Klein, I.; Dobrev, P.I.; Kottova, J.; Zazimalova, E.; Fekete, A.; Hartmann, A.; Schmitt-Kopplin, P.; Durner, J. Response of *Arabidopsis thaliana* to *N*-hexanoyl-DL: -homoserinelactone, a Bacterial Quorum Sensing Molecule Produced in the Rhizosphere. *Planta* **2008**, *229*, 73–85.
19. Bauer, W.D.; Mathesius, U. Plant Responses to Bacterial Quorum Sensing Signals. *Curr. Opin. Plant Biol.* **2004**, *7*, 429–433.
20. Fran, A. Characterizing Modified Celluloses Using Raman Spectroscopy. *Spectroscopy* **2016**, *31* (11), 22–27.

ACRONYMS AND ABBREVIATIONS

Acs	Acetobacter cellulose synthase
BNC	bacterial nanocellulose
2D	two dimensional
ΔC_n	relative correlation score
ΔM_{pep}	change in the mass of the peptide
DDHL	dodecanoyl homoserine lactone
DHL	decanoyl homoserine lactone
FDR	false discovery rate
FOV	field of view
HXHL	hexanoyl homo lactones
HS	Hestrin–Schramm
HSL	homoserine lactone
LC–MS/MS	liquid chromatography tandem mass spectrometry
MS	mass spectrometry
MS/MS	tandem mass spectrometry
<i>m/z</i>	mass-to-charge
NCBI	National Center for Biotechnology Information
ODDHL	oxydodecanoyl homoserine lactone
QS	quorum sensing
RSp	relative specificity
SEM	scanning electron microscope
Sp	specificity
Xcorr	correlation score

DISTRIBUTION LIST

The following individuals and organizations were provided with one Adobe portable document format (pdf) electronic version of this report:

U.S. Army Combat Capabilities
Development Command Chemical
Biological Center (CCDC CBC)
Detection Spectrometry Branch
FCDD-CBR-ID
ATTN: Jabbour, R.
Wade, M.

CCDC CBC Technical Library
FCDD-CBR-L
ATTN: Foppiano, S.
Stein, J.

Defense Technical Information Center
ATTN: DTIC OA

CCDC CBC Spectroscopy Branch
FCDD-CBR-IS
ATTN: Emmons, E.
Tripathi, A.



U.S. ARMY COMBAT CAPABILITIES DEVELOPMENT COMMAND
CHEMICAL BIOLOGICAL CENTER